



Research article

Simulation study on tractive performance of off-road tire based on discrete element method

Linxuan Zhou, Jingwei Gao*, Qiao Li and Cheng Hu

College of Aerospace Science and Engineering, National University of Defense Technology, Changsha 410072, China

* **Correspondence:** Email: gaojingwei@nudt.edu.cn.

Abstract: In order to improve the applicability and prediction accuracy of the existing simulation test methods of vehicle tractive performance on sandy soil, the off-road tire model using the discrete element method (DEM) under each operating condition is separately established in this paper. The contact parameters of DEM model are calibrated by rubber-sand friction test and soil bin test combined with corresponding simulation test. On this basis, the tire-sand simulation model is calculated under straight and inclining driving conditions, and the variation law of drawbar pull, torque, tractive efficiency and sinkage is obtained. This paper proves the feasibility of DEM simulation in studying vehicle tractive performance, and also provides a systematic parameter calibration method for improving the accuracy of DEM simulation, which is of great significance to enrich vehicle testing methods.

Keywords: off-road tire; tractive performance; sandy soil; discrete element method; numerical simulation; soil bin test

1. Introduction

In military and agricultural fields, the tractive performance of off-road vehicles have always been one of the key research objects. The indexes to evaluate tractive performance include drawbar pull, torque, tractive efficiency, sinkage, etc., which have an important impact on vehicle maneuverability under different ground conditions [1]. In the process of vehicle design and manufacturing, the tractive performance of tires is usually tested, so as to continuously improve the vehicle design [2]. However, how to test the tractive performance of tires under various driving

conditions is always a complex question.

In the field of vehicle terramechanics, tests are used to measure the tractive performance of tires in earlier studies, including outdoor real vehicle test and indoor soil bin test. However, there are some problems in the outdoor real vehicle test, such as high cost, complicated operation and difficult control of test conditions. At the same time, indoor soil bin test is limited by test instruments, and it is difficult to test heavy-load, large-size tires. In recent years, more and more researchers carried out tire tests through numerical simulation [3], among which the finite element method (FEM) and discrete element method (DEM) are widely used.

FEM is based on stress-strain relationships, including Bekker theory, Duncan model, Mohr-Coulomb failure criterion, etc.. These theoretical models assume sandy soil as a continuum model [4]. In fact, under the pressure and friction of tires, the sandy soil often deforms and breaks, presenting a discontinuous state, which is especially obvious under the action of high-speed and high-slip vehicles and in the extremely loose soil environment [5]. During this process, mechanical parameters such as Young's modulus and Poisson's ratio of sandy soil also change with the compression of soil pore space [6]. FEM based on the constant mechanics model lacks dynamic stability in the study of loose sandy soil, so it is more reasonable to adopt the discrete numerical simulation method for sandy soil [7].

DEM was originally proposed by Cundall [8,9] in 1971 to analyze discrete particle materials on the basis of molecular dynamics, and it was applied to discontinuous numerical studies such as geotechnical mechanics. DEM divides the macro sandy soil into a large number of independent particle models, and the contact relations between the particles are set up, including elasticity, friction, bonding, damping, etc., which can transfer pressure, shear and torque [10]. DEM can directly simulate the force and movement of all sandy soil particles under the action of external forces [11], and DEM conforms to the essence of discretization interaction of sandy soil particles [12]. Therefore, in this paper, DEM simulation is used to build the sandy soil model of multiple operating conditions, and then the law of tractive performance of off-road tires is studied.

Compared with FEM, DEM is more in line with the characteristics of discrete soil particles, so the Japanese scholar Oida [13] introduced it into the study of vehicle terramechanics in 2000, which started a new stage of numerical analysis of DEM in terramechanics. In 2002, Fujii [14] conducted a DEM simulation of the interaction between tires and soil, and made a comparative analysis of the simulation and test results. In 2003, Xu [15] used DEM to study machine-soil dynamics, and explored the advantages and disadvantages of DEM and improved it. In 2004, Nakashima [16] used DEM model to construct the soil surface and developed some sample programs to solve the basic tire-soil contact problems, which were proved to be of high accuracy. In 2006, Asaf [17] used DEM analysis software PFC2D to verify the early test of Oida [13]. In 2007, Nakashima [18] used the wall element and ball element in PFC2D software to construct the tire. Through the analysis, the abnormal increase of tractive performance of high-slip tire was obtained, which was not in accordance with the traditional classical theory, but was supported by subsequent tests and simulations. In 2008, Zou [19] used PFC2D to systematically study the interaction between tire and lunar soil under microgravity, laying a foundation for DEM research on vehicle terramechanics of China. In 2009, Zuo [20] used triangular mesh to divide soft soil into uniform discrete units, combined with soil viscoelasticity, plasticity and shear model, established the soil dynamics model, and realized the simulation of soil dynamic deformation.

In 2010, based on independent DEM particles, Koizumi [21] simulated soil particles of different

shapes and sizes by block command, and verified the soil model by soil bin test. In 2011, Wakui [22] established a three-dimensional tire-soil interactive model, and introduced the conditions of lug and contact geometry into the model. The simulation results of the tractive performance and the cornering were obtained. The model was proved to be accurate by test. In 2012, Wang [23] used two-dimensional DEM software to establish the interaction model between the tire and the soft ground, and made a simulation analysis of the interaction model. The feasibility of DEM in analyzing the interaction between tires and ground was verified. In 2013, Liu [24] and Zhang [25] established the dynamic simulation of three-dimensional tire of ostrich toe structure, and carried out the research on DEM bionic terramechanics. In 2014, Smith [26] compared DEM with terramechanics theory, and concluded that DEM had the best prediction effect on the analysis of vehicle tractive performance. Shi [27] constructed a low gravity field environment in PFC3D and discussed the effects of gravity field changes on the tractive performance of the lunar rover. Zhao [28] demonstrated the feasibility of coupling operation between sandy soil DEM model and tire FEM model, and improved the analysis efficiency of the model by subsection operations.

In 2015, Johnson [29] built the spherical particle unit in DEM software, and on this basis established the Mars soil model and carried out the research on the tractive performance of Mars rover. Combined with military background, Li [30] analyzed the influence of tire structure parameters on vehicle tractive performance in sandy environment. In 2017, Du [31] used PFC3D to simulate tire-sand interaction and analyze the influence of different lug effects on tractive performance. The analysis results showed that the intersection of lugs has no effect on tractive performance. Nishiyama [32] used the tire-sand DEM model controlled by proportional integral derivative (PID) to study the normal and tangential contact stresses of the tire. The applicability of the model was extended and the simulation results showed that the consistent angle of rotation for maximum normal contact stress and the maximum tangential contact stress shifts forward with the slippage increasing from 22%. In 2018, Kumar [33] evaluated the vertical deflection and contact area of 13.6–28 bias-ply and radial tires at different ballasted conditions. The results show that for all selected loads, the radial tire showed 13% higher contact area and 6.5% greater deflection than the bias-ply. Kumar [34] studied the deflection characteristics of radial-ply tires under different loads and inflation pressures and established an empirical model of radial tire deflection. The results showed that the model can be used to determine the optimal combination of normal load and inflation pressure to achieve the desired deflection. In 2019, Peters [35] established a vehicle-terrain simulation model by using DEM. According to the simulation results, the shear deformation, frictional resistance and expansion of soil under the action of vehicles were analyzed. The simulation results were compared with the existing vehicle performance database to prove the accuracy of the traditional drawbar pull test. However, there was still no reliable verification of contact parameter in the modeling process. Kumar [36] conducted tire tests under different ballast loads to study the average pulling ability and tractive power efficiency of radial tires. It is found that the maximum output power can be increased by ballast.

DEM has become one of the main research methods in the field of vehicle terramechanics, and DEM simulation based on tire-soil interaction has been applied to engineering practice [37]. However, there are still some limitations in DEM simulation of tire-soil interaction:

(a) The method of using DEM simulation to test the tire tractive performance is not mature enough. In particular, the numerical simulation model lacks reliable verification of contact parameter. This will lead to low precision of simulation parameters and large error of simulation results.

(b) The existing DEM simulation studies mainly focus on light vehicles, and the single-tire load is generally 50–500N. The studies on heavy-duty, large-size tires are scarce.

(c) The existing simulation research of vehicle terramechanics is mainly straight driving model, lacking of targeted and systematic research on longitudinal inclining, transverse inclining, horizontal inclining and other complex operating conditions.

Based on the above research status, the numerical simulation models of off-road tire and sandy soil are established in this paper. A method of systematically calibrating the contact parameters between tire and sandy soil model is proposed, that is, the contact parameters are calibrated through the friction test of sandy soil and the single-tire soil bin test combined with the corresponding simulation. After the modeling is completed, the tire traction simulation is carried out to calculate the drawbar pull, torque, tractive efficiency and sinkage. On this basis, the law of tractive performance of vehicles in multiple operating conditions is analyzed, which is of practical and innovative significance.

The structure of this paper is shown in Figure 1.

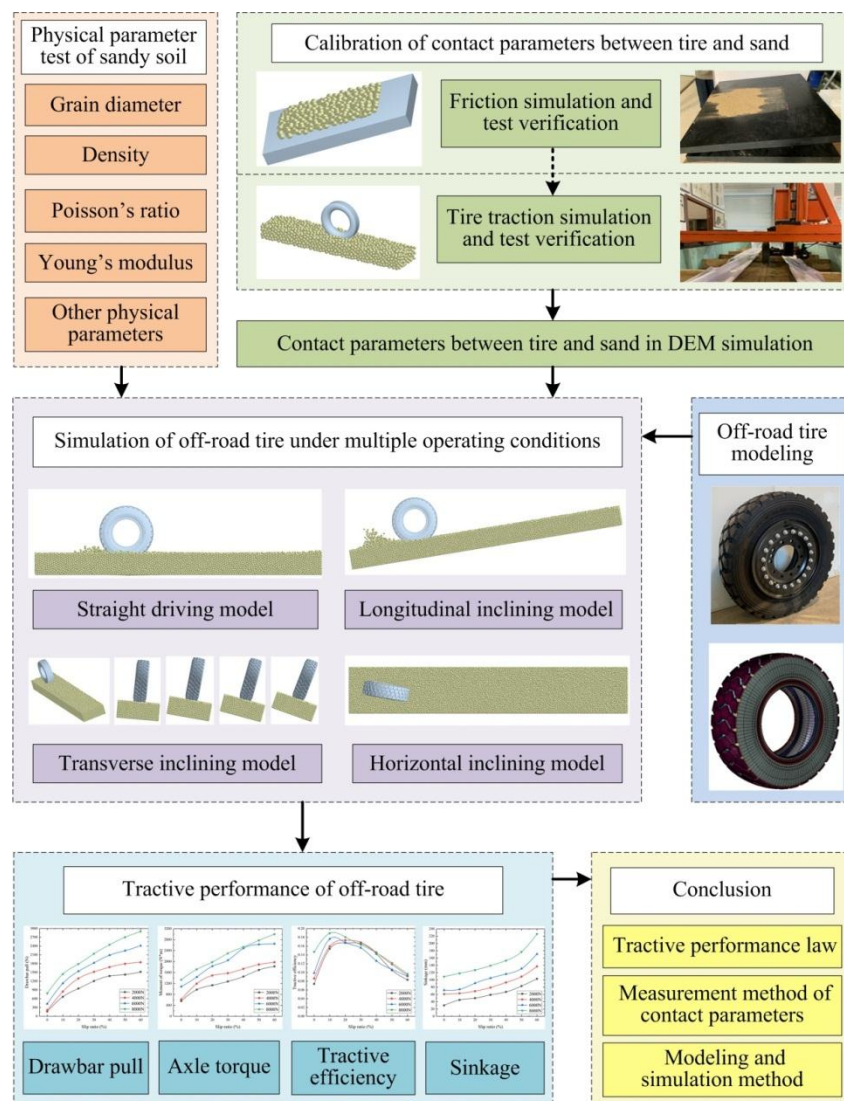


Figure 1. Schematic diagram for the structure of this paper.

2. Tractive performance theory of tire

In the driving process, the tractive performance of the tire are mainly embodied in the force provided by the soil, the torque consumption of the tire and the degree of subsidence of the tire on the soft soil surface. In this paper, the following four parameters are used as the evaluation indexes of tractive performance:

(a) Drawbar pull (F_{DP}): The force that the soil provides to the tire for its forward motion, that is, the difference between the soil thrust and the soil resistance.

(b) Axle torque (M): The center torque required for the tire to gain traction.

(c) Sinkage (z): The depth at which the tires sink in the elastic-plastic soil surface.

(d) Tractive efficiency (TE): The tractive efficiency is the ratio of the tractive power to the driving torque transferred from the engine to the tire. It comprehensively reflects the efficiency coefficient of the tractive capacity, torque consumption and forward speed.

The force analysis of off-road tire in the moving process is as follows:

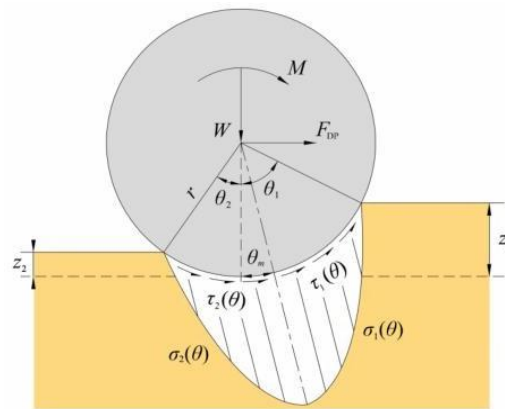


Figure 2. Mechanical model of tire-soil interaction.

In Figure 2, W is the tire load. θ , θ_1 , θ_2 and θ_m respectively represent the variable interaction angle, the approach angle, the leaving angle and the maximum stress angle. $\sigma(\theta)$ and $\tau(\theta)$ are separately the normal stress and the shear stress. z_1 is the sinkage in front of the tire and z_2 is the sinkage behind the tire. r is the rolling radius.

The formula of drawbar pull is as follows [38]:

$$F_{DP} = \frac{Db}{2} \int_0^{\theta_1} [\tau(\theta) \cos \theta - \sigma(\theta) \sin \theta] d\theta \quad (1)$$

Where, b and D are the width and diameter of the tire respectively.

The axle torque M is calculated as follows [39]:

$$M = M_S - M_R \quad (2)$$

M_S and M_R are respectively the driving couple provided by the engine and the friction couple provided by the ground during the driving process.

The calculation formula of tractive efficiency is as follows:

$$\text{T E} = \frac{F_{DP} \cdot r}{M} (1 - i) \quad (3)$$

Where, i is the slip ratio of tire, which reflects the relationship between the theoretical rotation speed $\omega_0 r$ and the actual forward speed v at a certain point on the tire. And the slip ratio is calculated by formula (4):

$$i = 1 - \frac{v}{\omega_0 r} \quad (4)$$

Where, ω_0 is the angular velocity of the tire; v is the actual forward speed of the tire.

According to Eq (3), tractive efficiency is related to drawbar pull, axle torque and slip ratio. When the slip ratio is constant, the tractive efficiency is proportional to the drawbar pull and inversely proportional to the axle torque.

In the slip sinkage model of Wong and Reece [40], the sinkage z is represented by two parts: static sinkage z_0 caused by soil compaction deformation and slip sinkage z_s caused by soil shear deformation. The formula is as follows:

$$z = z_0 + z_s = \left[\frac{3W}{(k_c + bk_\phi)(3-n)\sqrt{D}} \right]^{\frac{2}{2n+1}} + \frac{D}{2}(1-i)\theta_m \quad (5)$$

Where, k_c and k_ϕ are separately the cohesive modulus and internal frictional modulus of soil. n is the deformation index of soil. Compared with the sinkage calculation of soil mechanics, Wong-Reece model added slip sinkage. However, it is difficult to calculate θ_m in this model.

At present, the existing theory of tractive performance is not applicable to off-road tires with heavy load, large size and complicated tire pattern, and there is a lack of calculation and research on inclining driving model and other operating conditions. Therefore, it is necessary to carry out reliable numerical simulation to provide support for future theoretical research.

3. Conditions of numerical simulation

The research object of this paper is the tractive performance of the off-road tire on sandy soil. In the simulation system, mechanical parameters of tire and sandy soil, such as density, shear modulus and Poisson's ratio, need to be input. In addition, the contact parameters between the tire and the sandy soil, including restitution coefficient, static friction coefficient and rolling friction coefficient, need to be input in the simulation. These contact parameters can be obtained through a well-designed parameter calibration process.

3.1. Condition of tested tire and sandy soil

The off-road tire and simulation model studied in this paper are shown in Figures 3 and 4. The geometric and mechanical parameters of the tire are shown in Table 1.



Figure 3. The off-road tire.

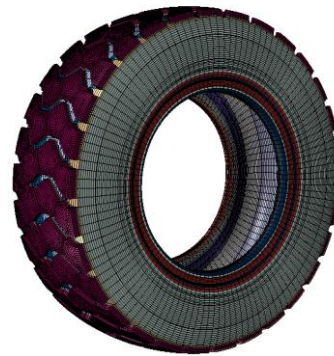


Figure 4. The simulation model of tire.

Table 1. The geometric and mechanical parameters of the tire.

Parameters/unit	Value
Rolling radius/mm	496
Outer perimeter/mm	3116
Width/mm	305
Height of lugs/mm	11
Rotating speed/rpm	10
Slip ratio/%	0,10,20,30,40,50,60

In order to measure the parameters of sandy soil, a series of tests were carried out, including density test, particle analysis test and triaxial compression test, as shown in Figure 5. These tests were conducted according to *Standard for Soil Test Method SL237-1999* [41], including *Article 4, Density Experiment, Article 6, Particle Analysis Experiment and Article 17, Triaxial Compression Test*.



(a) Density test



(b) Particle analysis test



(c) Triaxial compression test

Figure 5. The parameter measurement of sandy soil.

The mechanical parameters of sandy soil are shown in Table 2.

Table 2. Mechanical parameters of the sandy soil.

Parameter/unit	Value
Average grain diameter/mm	2.16
Density/kg·m ⁻³	2463.51
Young's modulus/MPa	31.75
Poisson's ratio	0.18
Internal friction angle/°	30.72
Internal cohesion/kPa	3.63
Moisture content/%	3.81

The above are the basic physical parameters of tire and sandy soil, which can be used for further modeling of tire-sandy soil.

Sandy soil model needs a large number of sandy soil particles. Computing speed is limited by the computer performance and number of particles. The general approach is to scale up the grain diameter of sandy soil particles and measure the contact parameters, so as to achieve the same effect as real sandy soil. This approach may cause difficulty in parameter calibration of the enlarged sandy particles. At present, there is no strict standard on the enlargement ratio of particle diameter in DEM simulation. Because the contact parameters will be calibrated after the diameter is enlarged, and the contact property of the enlarged particle can meet the research needs. According to the researches of other scholars, such as references [7,11,12,31,42–44], the diameter of DEM particles is usually within ten times enlargement, and the acceptable simulation results can still be obtained. After the preliminary research and simulation, the grain diameter of sandy soil model in this paper was finally determined to be 15–25 mm.

3.2. Calibration of contact parameters in DEM simulation

In DEM simulation modeling, it is very important to set accurate tire-sand contact parameters, including the recovery coefficient, static friction coefficient and rolling friction coefficient. These three coefficients have great influence on the accuracy of simulation results [45]. Users can access the contact parameters from the material database of the software EDEM, but the parameters in the material database can only estimate a general situation of ground. In order to evaluate specific ground conditions, a series of complex parameter calibration processes are required [46].

The parameter calibration process designed in this paper is as follows:

(a) Step-1: The friction test between tire rubber and sandy soil is conducted in laboratory.

(b) Step-2: A large number of friction simulation tests are carried out by setting different contact parameters. The contact parameters are assigned by orthogonal experimental design and range analysis. When the angle error between simulation and test is less than 5%, it can be considered that the contact parameters in the simulation are close to the correct value. There is more than one set of reasonable parameters, so the next verification is needed.

(c) Step-3: The several sets of reasonable contact parameters of Step-2 are respectively input into soil bin simulation test. The rotation speed and horizontal velocity of the tire were set by

RecurDyn software, and then the coupling simulation was carried out with the sandy soil in EDEM to calculate the drawbar pull and axle torque. Then the soil bin test is carried out to verify the simulation results. The contact parameters in the simulation with the minimum error are selected as the optimal parameters. These parameters can be used in off-road tire simulation model to simulate the real contact relationship between off-road tire and sandy soil.

3.2.1. Friction test and simulation

The total steps of the friction test are shown as below:

(a) Step-1: A square rubber board with the same material as the tire was prepared, the side length of the rubber board was 0.5 m. The rubber board was placed on the horizontal surface of the table.

(b) Step-2: In the center of the rubber board, the sandy soil with a side length of 200 mm and a thickness of 2 mm was placed evenly, as shown in Figure 6a.

(c) Step-3: One side of the rubber board was lifted slowly until the sandy soil began to slide, as shown in Figure 6b. The angle between the rubber board and the horizontal table was measured as the test result.

The measured angle was determined by the contact relationship between the sandy soil and the tire rubber, so the friction test could be used as a parameter calibration method to obtain the contact parameters in DEM simulation.

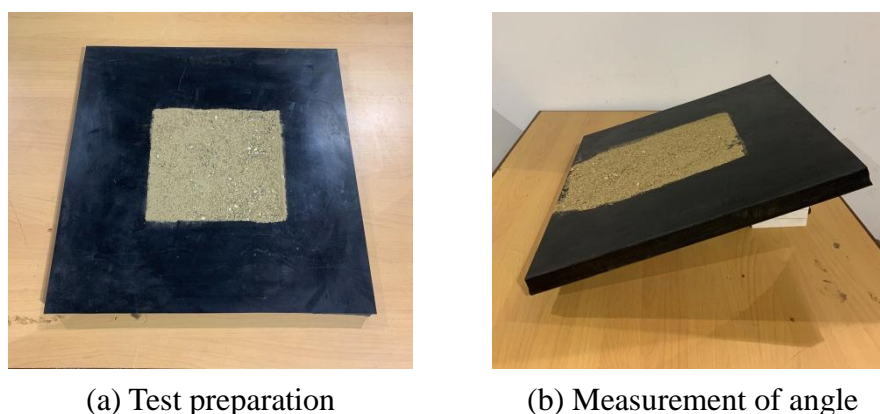


Figure 6. Process of friction test.

Through the test, the inclination angle of the rubber board was 31.47° when the sandy soil began to slide. The next step is the simulation test of sandy soil model and rubber board model.

In simulation software EDEM, the same simulation model was established according to the friction test. A large number of different contact parameters were input for simulation test, and the simulation time step was 1×10^{-5} s. The simulation process is shown in Figure 7.

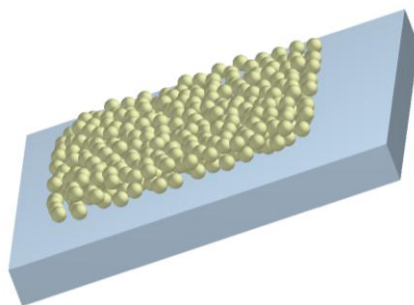


Figure 7. Process of friction simulation test.

After each simulation, the angle results of numerical simulation and friction test were compared. When the angle measured by the simulation was the same as the test, the contact relationship was close to the right one. In order to reduce the workload and get the results consistent with the test as soon as possible, the orthogonal experimental design and range analysis were used to assign the contact parameters. Finally, four sets of contact parameters with the minimum error were obtained, as shown in Table 3.

Table 3. Results and error of friction simulation tests.

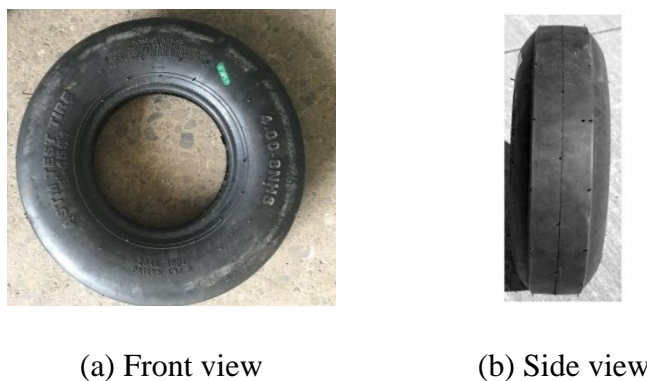
	(a)	(b)	(c)	(d)
Restitution coefficient	0.56	0.47	0.63	0.46
Static friction coefficient	0.52	0.57	0.49	0.41
Rolling friction coefficient	0.41	0.35	0.48	0.59
Simulation result/°	31.13	31.71	32.27	30.87
Test result/°	31.47	31.47	31.47	31.47
Error/%	1.08	0.76	2.54	1.91

In the case of these four sets of contact parameters, the results of friction test and simulation are very similar, and the error is within 3%. It is necessary to conduct the soil bin test and simulation to determine the final correct contact parameters.

3.2.2. Tire traction simulation and soil bin test

In order to further verify which set of parameters in Table 3 could accurately describe the contact effect of tire and sandy soil, this section conducted simulation of tire linear traction according to the four sets of contact parameters in Table 3, and calculated the results of traction and torque. At last, the results of soil bin test verified the simulation to determine the accurate contact parameters.

The size of the off-road tire studied in this paper are large, and the existing test equipment cannot support the test. Therefore, a smooth tire with the same material and physical properties but a smaller size was designed and manufactured, as shown in Figure 8. The tire has a rolling radius of 0.25 m and a width of 0.1 m. Considering the condition of heavy load and test equipment, the normal load was determined to be 1000 N. Tests and simulations were conducted to verify which set of contact parameters between the tire rubber and sandy soil was the most accurate.

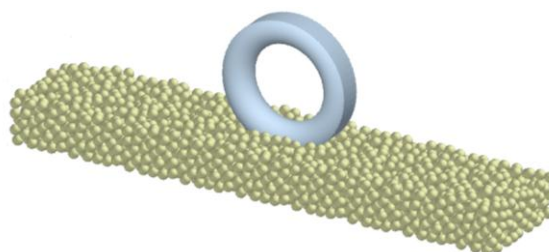


(a) Front view

(b) Side view

Figure 8. The tire for soil bin test.

The tire traction simulation was conducted by the coupling simulation of DEM simulation software EDEM and multi-body dynamics software RecurDyn. The sandy soil model was established in EDEM, with the length, width and height of 6 m, 0.5 m and 0.4 m respectively. Import the tire in RecurDyn into EDEM. The tire model was modeled in RecurDyn and imported into EDEM. The physical parameters and contact parameters were input into the software, the tire slip ratio was set from 0 to 60%, the load was 1000 N, and the time step was 2×10^{-5} s. The simulation process is shown in Figure 9.

**Figure 9.** Tire traction simulation.

The results of drawbar pull and torque were obtained by simulation. The next step is to verify the simulation results by the soil bin test. And the results of simulation and test will be plotted together for comparison.

The equipment of soil bin test is independently designed, including the main body of soil bin, the loading facilities, the driving system and sensor, as shown in Figures 10 and 11. The size of the equipment is 9000 mm \times 500 mm \times 200 mm. The equipment can set the tire speed and forward speed, and the required data in the whole traction process are collected by the sensor. The sensor used in the soil bin test is the six-axis force/torque sensor of ATI industrial automation company, the model is FC-OMEGA160, as shown in Figure 11b.

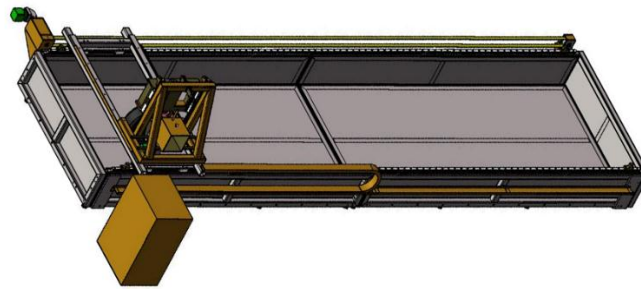
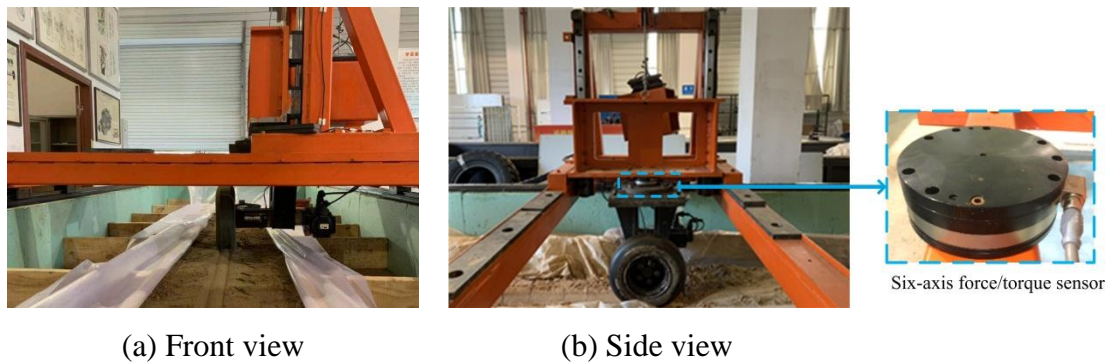


Figure 10. The schematic diagram of soil bin test



(a) Front view

(b) Side view

Figure 11. The equipment for soil bin test.

After the tire were fixed on the driving system and the tire load was set to 1000 N, the driving system was turned on and the test began. The value of drawbar pull and torque of tire under different slip ratio was measured. The test process is shown in Figure 12.



Figure 12. The tire indentation formed during the test.

After the test was completed, the results of drawbar pull and torque were denoised and compared with the results of the simulation, as shown in Figure 13.

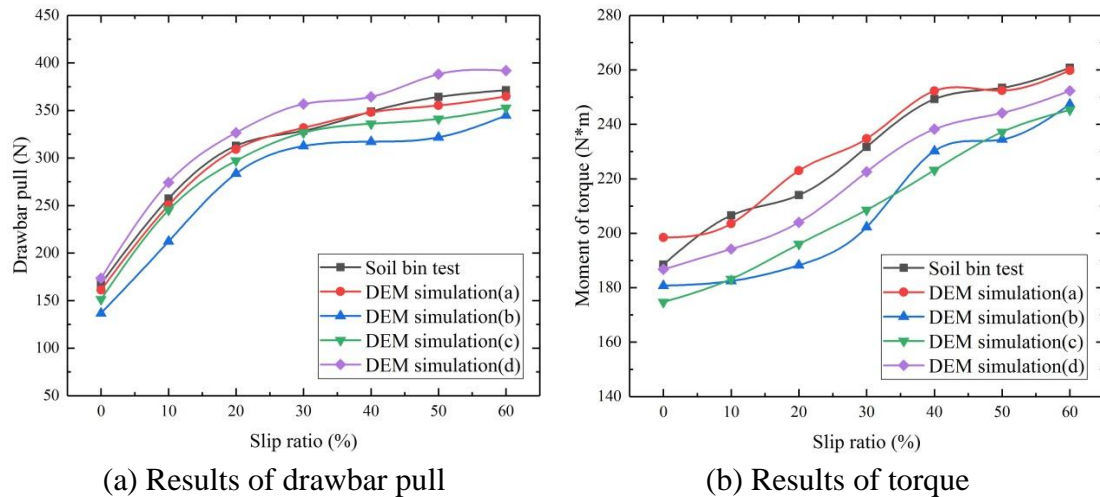


Figure 13. Simulation and test results of smooth tire.

According to the results of test and simulation, the error of simulation results under different contact parameters was calculated, as shown in Table 4.

Table 4. The error of simulation results.

Simulation	Average error of drawbar pull/%	Average error of torque/%
(a)	1.88	2.03
(b)	11.17	8.68
(c)	5.01	8.54
(d)	5.63	3.83

It can be seen from the test and simulation that the contact parameters between tire and sandy soil have different effects on the drawbar pull and torque. The error trends of drawbar pull and torque are also different when the contact parameters are changed. Because the contact parameters also change the friction between the tire and the ground in the simulation. In the case of simulation (a), the calculated traction performance results are closer to the results of the soil bin test, and the error of drawbar pull and torque are both the minimum and within 3%, meeting the accuracy requirements. Therefore, the restitution coefficient, static friction coefficient and rolling friction coefficient between the tire and the sandy soil are determined to be 0.56, 0.52 and 0.41, respectively, as the parameters for the next off-road tire simulation.

4. Simulation of off-road tire under multiple operating conditions

After the parameter calibration and verification in chapter 2 and chapter 3, the parameters needed for off-road tire simulation were finally determined. This chapter established the simulation model of off-road tire traction on sandy soil under multiple operating conditions, and calculated the tractive performance of the off-road tire. Four typical operating conditions, including straight, longitudinal inclining, transverse inclining and horizontal inclining, were selected for analysis.

4.1. Straight driving model

The numerical simulation model of sandy soil was established. A total of 44400 sandy particles were produced automatically by particle factories in EDEM. Under the action of gravity, all particles collided and consumed energy in the cuboid area to reach the equilibrium state, that is, the sandy soil model. The RecurDyn model of off-road tire was imported into EDEM to complete the numerical simulation modeling of straight driving, as shown in Figure 14. The length, width and depth of sandy soil were 6 m, 1 m and 0.4 m respectively.

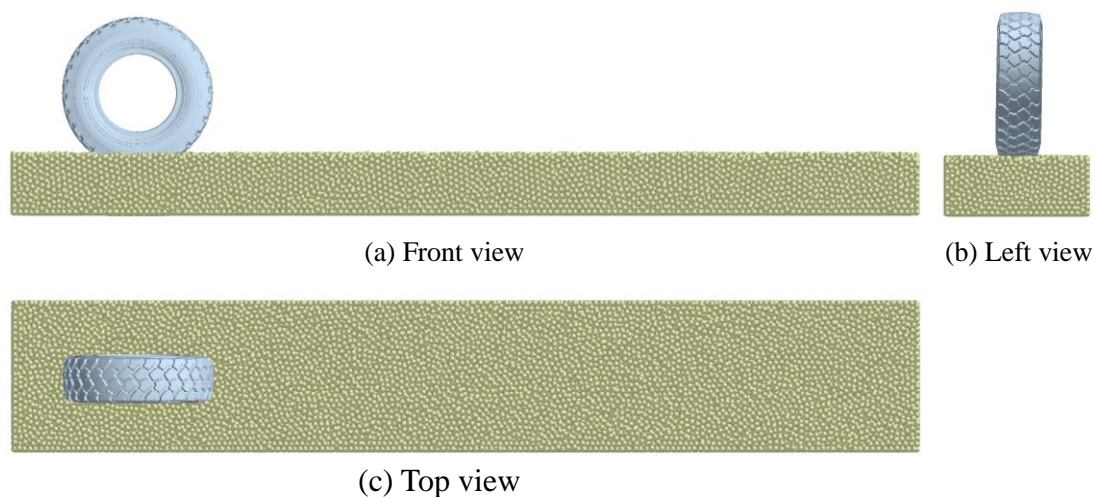


Figure 14. Numerical simulation model of straight driving.

Tire load and slip ratio were set by RecurDyn and coupled with EDEM for simulation. The simulation time step is 5×10^{-5} s, and the simulation process is shown in Figure 15.

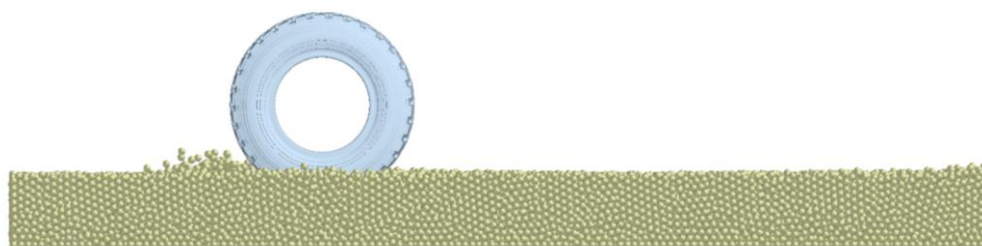


Figure 15. The simulation process of straight driving.

The traction simulation of off-road tire under the load of 2000 N, 4000 N, 6000 N and 8000 N was carried out respectively. The results of drawbar pull, torque, tractive efficiency and sinkage of the off-road tire were calculated through the simulation. Where, the drawbar pull of the tire is the traction value in its driving direction, and the torque is the moment of the tire in the rotation direction. The simulation results are shown in Figure 16.

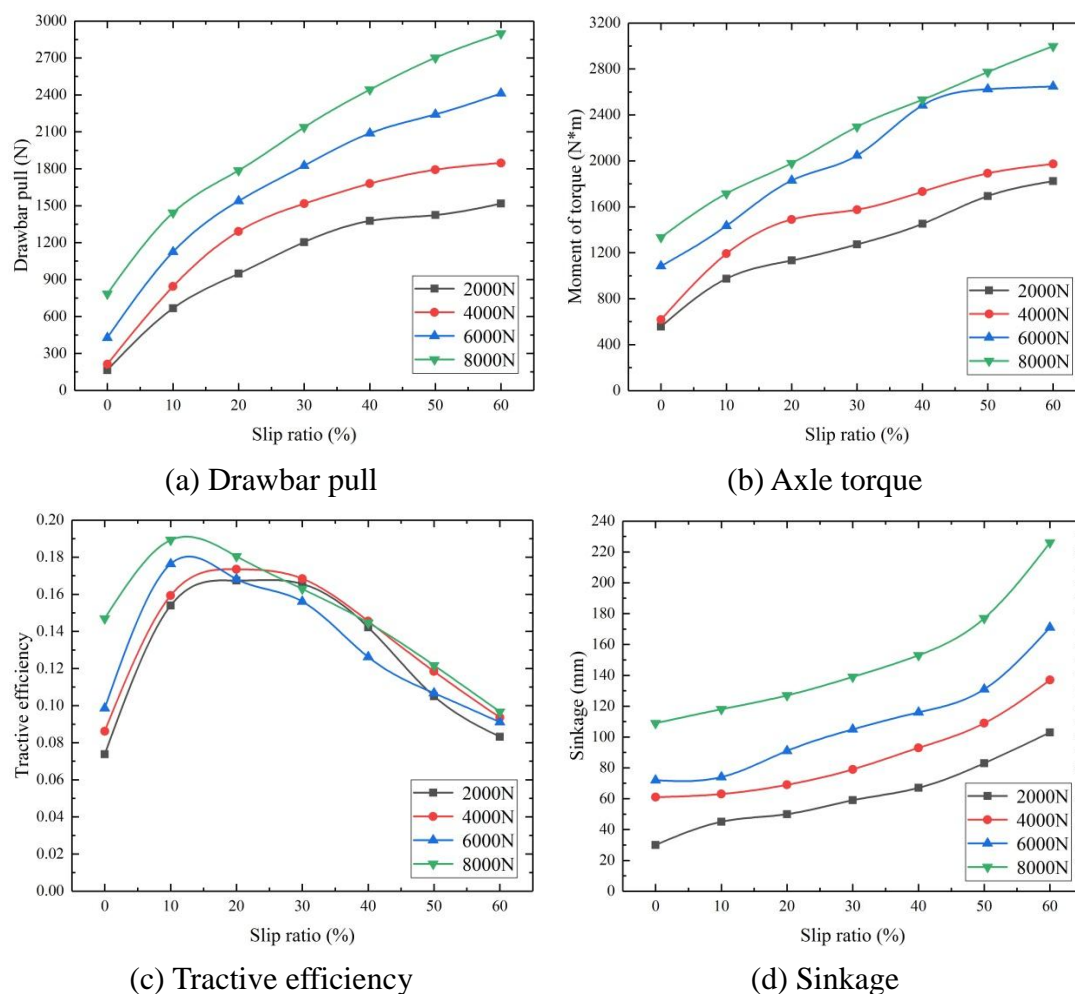


Figure 16. Simulation results of straight driving model.

As can be seen from Figure 16a, with the increase of tire load, the drawbar pull significantly increases. The drawbar pull increases linearly with the increase of vertical load, and the rising slope with low slip ratio is close to that with high slip ratio. In addition, the load has a greater influence on the simulation results at high slip ratio.

According to Figure 16b, the axle torque increases linearly with the increase of vertical load. The torque also increases with the increase of the slip ratio. At the low slip ratio of less than 30%, the rising slope of torque is greater than that at the high slip ratio of more than 40%. There is some fluctuation in torque variation. The reason is that the friction between the tire and sandy soil fluctuates when the tire is running, which affects the driving torque needed to control the tire speed.

In Figure 16c, with the increase of slip ratio, the tractive efficiency shows a tendency of first rising and then decreasing. The tractive efficiency of 2000 N load reaches the peak at about 25% slip ratio, the peak efficiency of 4000 N load is about 20% slip ratio, and the peak efficiency of 6000 N and 8000 N load is about 15% slip ratio. Therefore, it can be considered that with the continuous increase of tire load, the peak value of tractive efficiency moves to the direction of low slip ratio. This also shows that when the vehicle is off-road driving, keeping a proper slip ratio can ensure the full use of energy while ensuring the speed. In the case of low slip ratio, with the increase of tire load, the tractive efficiency rises first. After the load exceeds 6000 N, the rising trend increases

significantly, tending to 0.15 efficiency value. However, in the case of high slip ratio, the efficiency coefficient is little affected by tire load.

Under the condition of low slip ratio, the tractive efficiency is mainly related to the drawbar pull and axle torque. The drawbar pull increases significantly with the increase of the slip ratio, and the increase rate is larger than that of the axle torque, thus promoting the increase of the tractive efficiency. When the slip ratio increases to a certain extent, the tractive efficiency reaches its peak. If the slip ratio continues to increase, it will have a greater effect on tractive efficiency than the drawbar pull, resulting in a decrease in tractive efficiency.

Figure 16d shows the change curve of sinkage with slip ratio. It can be found that the sinkage shows a linear upward trend with the increase of vertical load, but the upward slope at a high slip ratio of more than 40% is significantly greater than that at a low slip ratio of less than 30%.

To sum up, the variation trend of various tractive performance indexes of tire is basically the same under different load. The increase of the vertical load will lead to the linear increase of the drawbar pull, axle torque and sinkage, and promote the peak tractive efficiency to move towards the direction of low slip ratio. In straight driving condition, the DEM simulation model in this paper has good applicability.

4.2. Longitudinal inclining model

In addition to the typical straight driving condition, off-road vehicles often experience the condition of longitudinally inclined ground, that is, the popular climbing condition. According to the same modeling principle as in section 4.1, sandy soil with different longitudinal inclining angles was established in EDEM, and the inclining angles were 5° , 10° , 15° and 20° respectively. The off-road tire model was placed on the surface of the sandy soil model. In order to prevent the action of the inertial force inside the model caused by the instantaneous load, the vertical load of 4000 N was gradually applied to the center of the tire model. After the modeling was completed, the simulation time step was set to 5×10^{-5} s for coupling simulation, as shown in Figure 17.

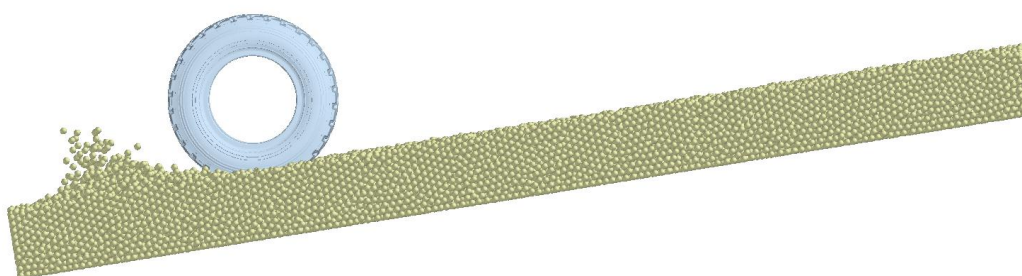


Figure 17. The simulation process of longitudinal inclining driving.

Through the simulation calculation, the law of tractive performance of off-road tire under the longitudinal inclining condition is calculated, as shown in Figure 18.

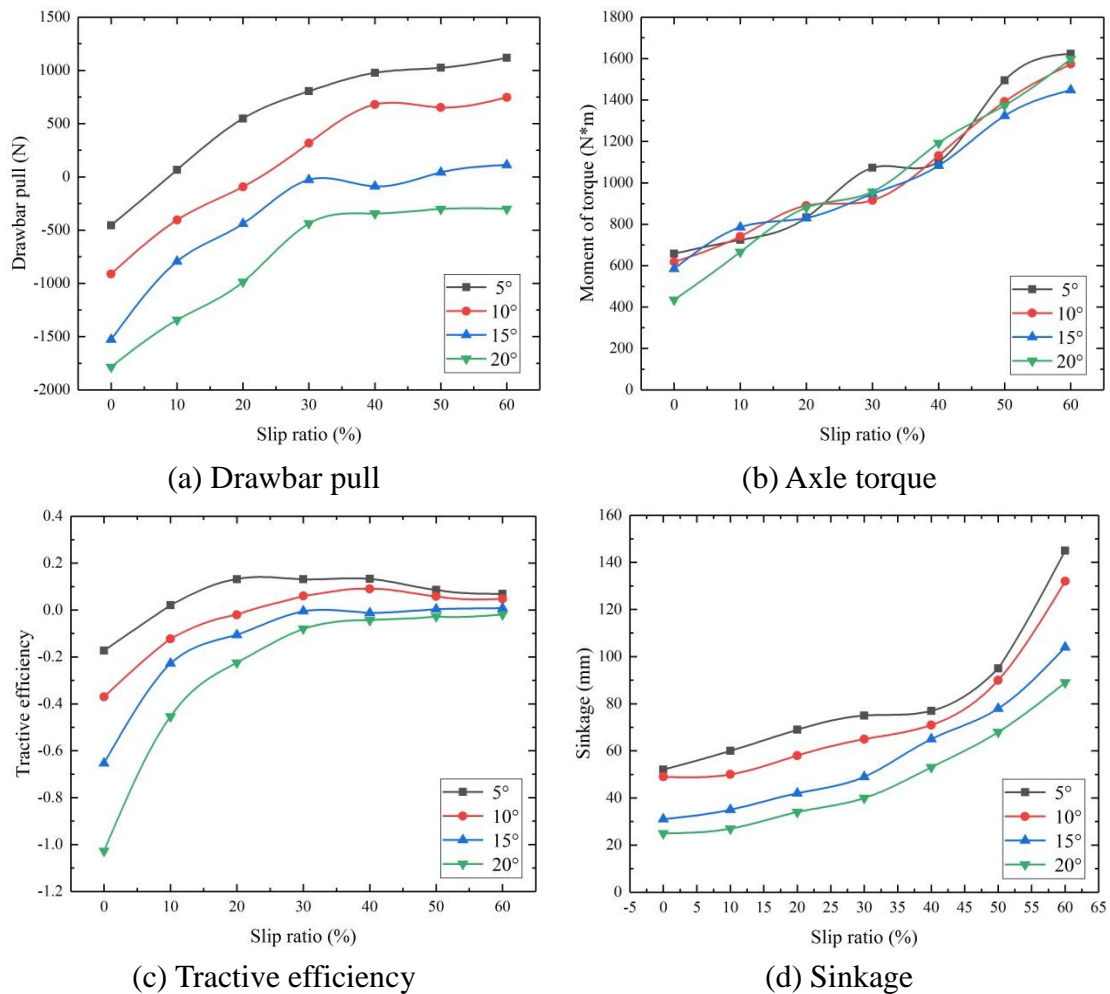


Figure 18. Simulation results of longitudinal inclining model.

Figure 18a shows the change curve of drawbar pull under different longitudinal inclinations of ground. It can be seen that with the increase of the inclination angle, the drawbar pull presents a completely linear downward trend, and the decline under the condition of 20% low slip ratio is very close to that under the condition of 50% high slip ratio. With the increase of the slip ratio, the increasing trend of the drawbar pull gradually slows down, which also indicates that when the vehicle climbs the slope, it is limited to obtain traction by increasing the speed.

According to Figure 18b, the effect of longitudinal inclination on torque is small, and the difference of results under different longitudinal inclination angle is not obvious. The comparison analysis of the torque under the condition of 20% low slip ratio and 50% high slip ratio is as follows: the simulation value of torque shows a slight decrease with the increase of the inclination angle, and the change characteristics of high slip ratio and low slip ratio are basically the same. The numerical simulation results fluctuate greatly, and the torque under the condition of high slip will rise abnormally when the longitudinal inclination angle of the ground is 20°.

In Figure 18c, the influence of ground inclination angle on tractive efficiency is significant, and the variation curves of efficiency under different angle conditions are highly differentiated. When the longitudinal inclination angle is 5°, the peak efficiency appears around 20% slip ratio, while when the longitudinal inclination angle is 10° and 15°, the peak efficiency appears around 30–40% slip

ratio. The peak efficiency is no longer obvious when the longitudinal inclination angle continues to increase. With the increase of the inclination angle, the tire tractive efficiency presents a linear attenuation trend. Different from other operating conditions, the decreasing trend of efficiency under low slip ratio is significantly greater than that under high slip ratio. After the inclination angle is greater than 10° , the efficiency drops to negative value, with no tractive performance at all. On the other hand, with the increase of the inclination angle, the efficiency under the condition of low slip ratio decreases sharply.

Figure 18d reflects the variation range of the sinkage under different longitudinal inclining conditions. It can be found from the curves that: The variation range of sinkage is small at low slip ratio, but large at high slip ratio. On the whole, the sinkage decreases with the increase of the longitudinal inclination angle, and the decreasing trend under the condition of high slip ratio is slightly greater than that under the condition of low slip ratio.

4.3. Transverse inclining model

The transverse inclining driving usually occurs when the vehicle runs, such as the lateral driving on the slope and the obstacle crossing on one side. Off-road vehicles, in particular, need to cope with more complex ground conditions. According to the typical transverse inclining condition, the numerical models of the ground under the lateral inclination angle of 5° , 10° , 15° and 20° were set respectively. As shown in Figures 19 and 20.

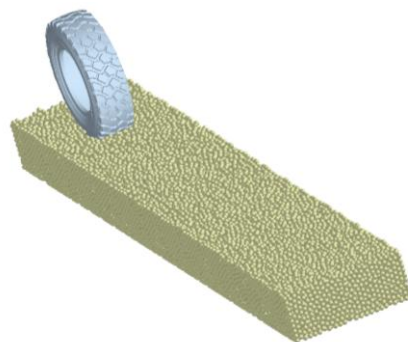


Figure 19. Numerical simulation model of transverse inclining driving.

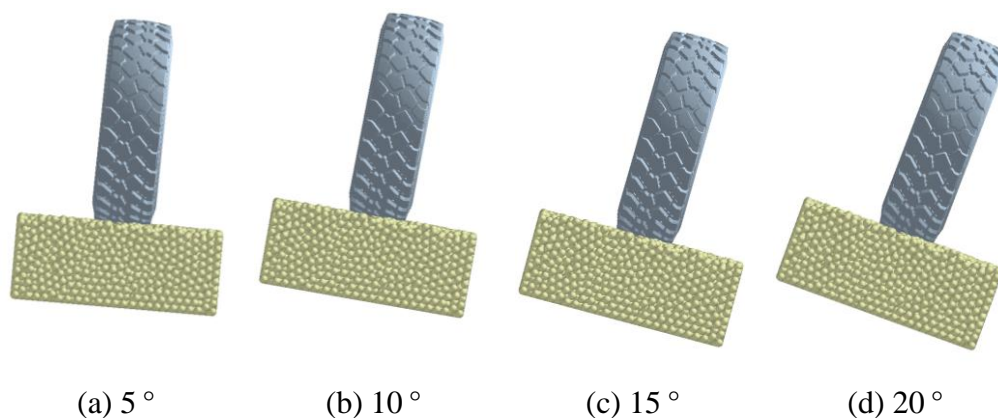


Figure 20. Left view of the simulation model with different inclination angles.

After the simulation settings were completed, the results of tractive performance were calculated as shown in the figure below.

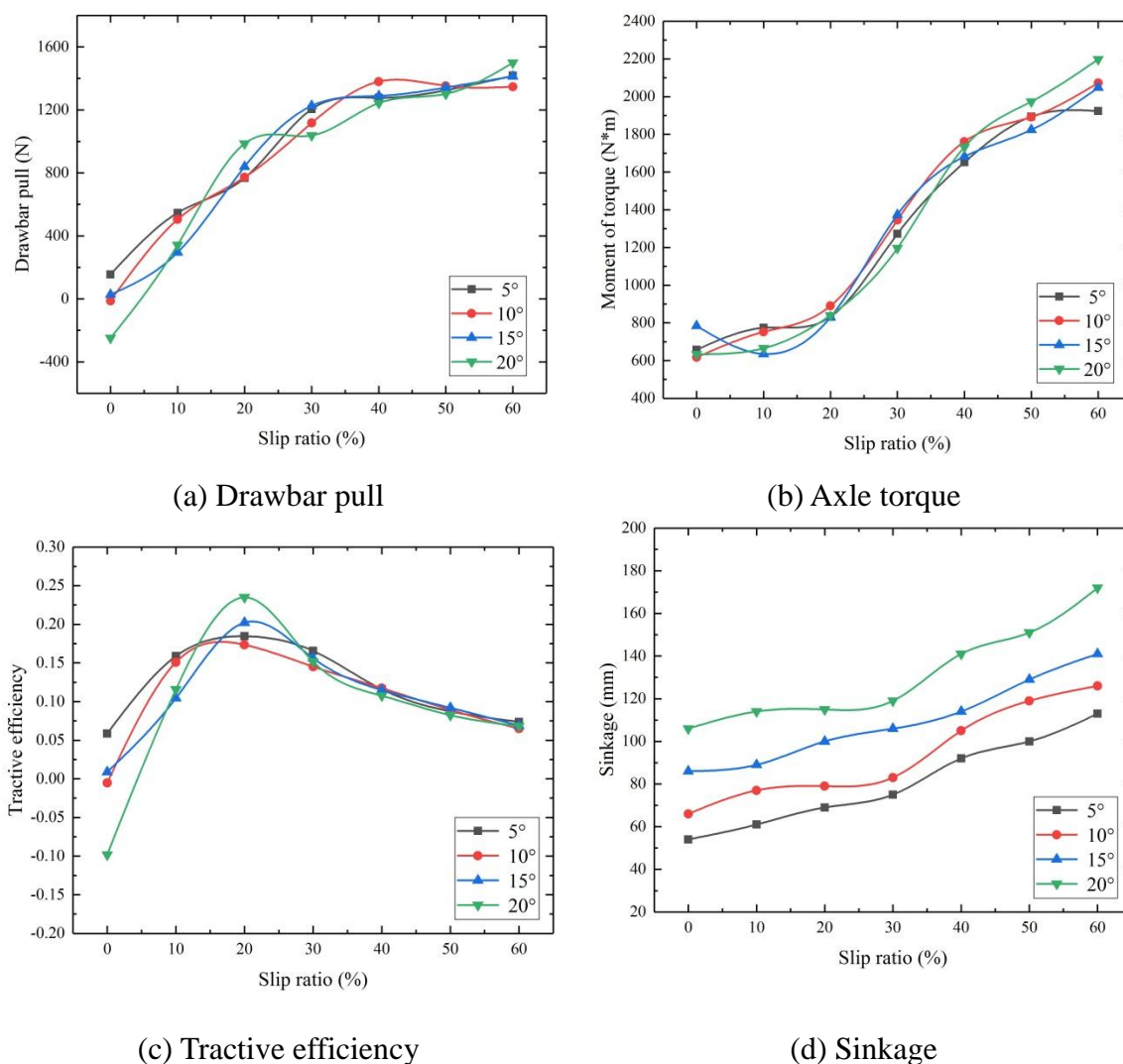


Figure 21. Simulation results of transverse inclining model.

It can be seen from the curve of drawbar pull in Figure 21a that the influence of transverse inclining on the tire drawbar pull is not significant, and the drawbar pull curve under different inclination conditions is not clearly discernible. Therefore, a comparative analysis is made on the drawbar pull under the conditions of 20% low slip ratio and 50% high slip ratio, indicating that the drawbar pull slightly decreases with the increase of the transverse inclining angle. The simulation results of drawbar pull increase with the increase of slip ratio, and the increase gradually slowed down with fluctuation.

Figure 21b shows the variation curve of torque with slip ratio in the numerical simulation, which is similar to the variation characteristics of drawbar pull. The difference of torque curves under different transverse inclining conditions is not obvious. The simulation results show a similar increasing trend with the increase of the ground inclination angle. At the condition of 20% low slip ratio, the torque reaches the minimum value when the inclination angle is 5°, and then presents an

upward trend. Under the condition of 50% high slip ratio, the torque reaches the minimum value when the inclination angle is 15° , and then continues to rise. The above trend is similar to the situation of drawbar pull.

In Figure 21c, the tractive efficiency of different transverse inclining conditions reach the peak at about 20% of the slip ratio, and the change curves after that are almost identical. The influence of transverse inclining angle on tractive efficiency is very small. When the slip ratio is higher than 30%, the tractive efficiency almost does not change with the inclination angle. Under the condition that the slip ratio is less than 20%, the results of tractive efficiency fluctuate greatly, but there is no obvious correlation between the variation law and the inclination angle.

According to Figure 21d, the sinkage of tire is the minimum at 5° transverse inclining angle, and then continues to rise with the increase of angle. The variation trend is more obvious when the slip ratio is more than 40%.

To sum up, the transverse inclining condition of ground will promote the significant increase of tire sinkage, weaken the tire drawbar pull and torque to some extent, and have little influence on the tractive efficiency of tire.

4.4. Horizontal inclining model

Horizontal inclining is also a very common driving condition of vehicles. When the vehicle encounters lateral force such as transverse wind or multi-axis steering, the rolling direction of the tire will produce a certain angle with its forward direction, that is, the horizontal inclining angle. In order to simulate the horizontal inclining effect of the tire in the driving process, based on the straight driving model, this section kept the forward direction of the tire model unchanged, and set the model to rotate 5° , 10° , 15° and 20° respectively around the vertical axis to form horizontal inclining angle. The numerical simulation model of horizontal inclining driving condition, as shown in Figure 22, was established.

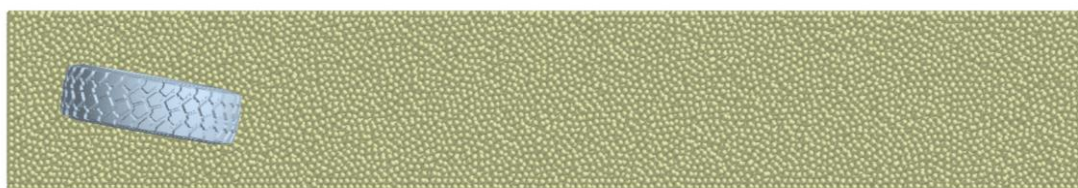


Figure 22. Numerical simulation model of horizontal inclining driving.

The simulation results of Horizontal inclining model are shown in Figure 23.

In Figure 23a, with the increase of horizontal inclining angle, the results of drawbar pull show a linear downward trend, and the trend is more obvious in high slip ratio condition. The simulation results reach the peak value at 5° horizontal inclining angle under high slip condition and decrease significantly with the increase of inclining angle. The reason for the above changes is that the horizontal inclining bulldozing area overlaps with the area in the forward direction of tire, resulting in the repeated calculation of the additional resistance of the horizontal inclining bulldozing. When the horizontal inclining angle is small, the area of the bulldozing is small and the response to the slip

ratio is not obvious. With the increase of angle, the area of bulldozing area increases, and the drawbar pull is obviously affected by the slip ratio.

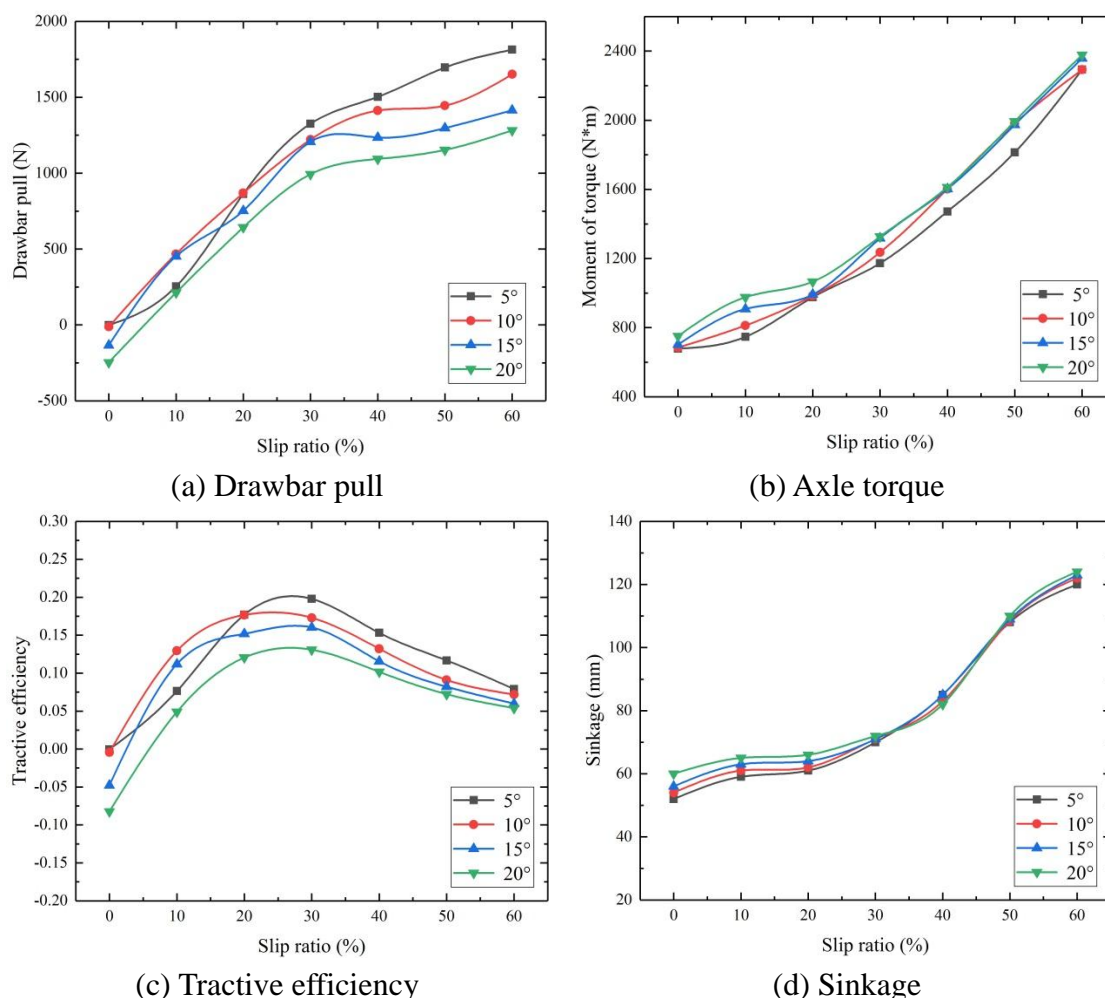


Figure 23. Simulation results of horizontal inclining model.

It can be seen from Figure 23b that the influence of horizontal inclining angle on torque is not significant, and the torque change curves under different inclining conditions basically coincide. The comparison of torque under the conditions of 20% low slip ratio and 50% high slip ratio found that: The simulation results are almost unchanged with the increase or decrease of the horizontal inclining angle, and are in a small range of fluctuation state. It can be considered that the tire torque is not affected by the horizontal inclining angle.

As can be seen from Figure 23c, in the horizontal inclining condition, the tractive efficiency first increases and then decreases with the increase of slip ratio. A comparative analysis of the tractive efficiency under low slip ratio and high slip ratio shows that the efficiency decreases linearly with the increase of horizontal inclining angle, and the decreasing trend is more significant under the high slip ratio condition.

Figure 23d shows the change curve of sinkage with slip ratio calculated by simulation. The simulation results show that the tire sinkage is little affected by the horizontal inclining angle, and the sinkage curves are almost identical under different horizontal inclining conditions. Only in the

case of low slip ratio, the sinkage increases slightly with the increase of inclining angle

To sum up, the horizontal inclining simulation model of off-road tire established in this chapter is applicable in horizontal inclining driving, which reflects the phenomenon that the drawbar pull is weakened by horizontal inclining of the tire, and horizontal inclining driving has little effect on torque and sinkage.

5. Conclusions

In view of the problems existing in the DEM simulation test method for tractive performance of off-road tire, a systematic parameter calibration method for the DEM simulation model of tire-soil was proposed. The contact parameters between tire and sandy soil were evaluated, and the accuracy of the DEM model was verified. The tire-soil simulation model under multiple operating conditions was established to test the tractive performance. It could be concluded that:

(a) Under straight driving condition, the increase of tire load can cause the increase of drawbar pull, torque and sinkage in different ranges, and promote the peak tractive efficiency to move towards the direction of low slip ratio. Drawbar pull increases with the increase of slip ratio, while the tractive efficiency increases first and then decreases gradually. In particular, when the slip ratio increases from 0 to 20%, the drawbar pull increases significantly.

(b) The longitudinal inclining driving condition will result in linear reduction of the drawbar pull, torque, sinkage and tractive efficiency of the tire to varying degrees. When the slip ratio is 0–30%, the effect of longitudinal inclining condition on drawbar pull and traction efficiency is greater than other tractive performance indexes, while when the slip ratio is higher than 30%, the effect on sinkage is more obvious.

(c) The influence of the transverse inclining operating condition on the drawbar pull and torque of the off-road tire is small, but the tire sinkage is significantly increased. The increase of the transverse inclination angle will promote the peak tractive efficiency to move toward the direction of high slip ratio, which is manifested in that the slip ratio gradually approaches from 15 to 20%. When the slip ratio is large, the inclination angle has little effect on the tractive efficiency.

(d) The horizontal inclining working condition significantly reduces the drawbar pull and tractive efficiency of the off-road tire. In the case of high slip ratio, the influence of tire horizontal inclination angle on drawbar pull is more significant. The horizontal inclination angle has little influence on the torque and sinkage. For every 5° increase in inclination angle, torque and sinkage increase by less than 5%.

Acknowledgments

This paper is sponsored by National Key Research and Development Program (No. 2017YFB1300900), Chinese National Natural Science Foundation (No. 51605483), and Science Foundation of National University of Defense Technology (No. ZK17-03-02, No. ZK18-03-55).

Conflicts of interest

The authors declare no conflict of interest in this paper.

References

1. Y. Du, J. Gao, L. Jiang, Development and numerical validation of an improved prediction model for wheel-soil interaction under multiple operating conditions, *J. Terramech.*, **79** (2018), 1–21.
2. Y. Zhang, J. Gao, Q. Li, Experimental study on friction coefficients between tire tread rubber and ice, *AIP. Adv.*, **8** (2018), 075005.
3. Y. Zhang, J. Gao, Q. Li, Study on tire-ice traction using a combined neural network and secondary development finite element modeling method, *Concurr. Comp. Pract. E.*, **31** (2019), e5045.
4. I. C. Schmid, Interaction of vehicle and terrain results from 10 years research at IKK, *J. Terramech.*, **32** (1995), 3–26.
5. M. Momozu, A. Oida, M. Yamazaki, Simulation of a soil loosening process by means of the modified distinct element method, *J. Terramech.*, **39** (2002), 207–220.
6. F. Koichiro, U. Masami, H. Koichi, Mathematical models for soil displacement under a rigid wheel, *J. Terramech.*, **43** (2006), 287–301.
7. W. Smith, H. Peng, Modeling of wheel-soil interaction over rough terrain using the discrete element method, *J. Terramech.*, **50** (2013), 277–287.
8. P. A. Cundall, *The Measurement and Analysis of Acceleration on Rock Slopes*, Doctoral dissertation, University of London, 1971.
9. P. A. Cundall, In *A computer model for simulating progressive large scale movements in blocky rock systems*, Proceedings of the Symposium of the International Society of Rock Mechanics, France, 1 (1971), 8–12.
10. J. Li, Y. Zhang, J. Zhou, Study on prediction method of the sinkage of track with big shoes, *Agri. Equip. Veh. Eng.*, **51** (2013), 33–36.
11. F. Dai, X. Song, W. Zhao, F. Zhang, H. Ma, M. Ma, Simulative calibration on contact parameters of discrete elements for covering soil on whole plastic film mulching on double ridges, *Trans. Chin. Soc. Agri. Mach.*, **50** (2019), 50–56.
12. X. Wang, H. Hu, Q. Wang, H. Li, J. He, W. Chen, Calibration method of soil contact parameters based on DEM theory, *J. Agri. Mach.*, **48** (2017), 78–85.
13. A. Oida, S. Ohkubo, In *Effect of tire lug cross section on tire performance simulated by distinct element method*, Proceedings of 13th International Conference of ISTVS, (1999), 345–352.
14. H. Fujii, A. Oida, H. Nakashima, In *Analysis of Interaction between lunar terrain-wheel and treaded wheel by distinct element method*, Proceedings of 14th International Conference of ISTVS, (2002), 323–328.
15. Y. Xu, Modeling and methodological strategy of discrete element method simulation for tillage soil dynamics, *Trans. Chin. Soc. Agri. Eng.*, **19** (2003), 34–37.
16. H. Nakashima, A. Oida, Algorithm and implementation of soil-tire contact analysis code based on dynamic FE-DE method, *J. Terramech.*, **41** (2004), 127–137.
17. Z. Asaf, D. Rubinstein, I. Shmulevich, Evaluation of link-track performances using DEM, *J. Terramech.*, **43** (2006), 141–161.
18. H. Nakashima, H. Fujii, A. Oida, M. Momozu, Y. Kawase, H. Kanamori, et al., Parametric analysis of lugged wheel performance for a lunar microrover by means of DEM, *J. Terramech.*, **44** (2007), 153–162.

19. M. Zou, *Study on Traction Ability for Driving Wheel of the Lunar Rover*, Doctoral dissertation, Jilin University, 2009.
20. Y. Zuo, Dynamic modeling and application of soil for vehicle terramechanics, *J. Lanzhou. Univ.*, **45** (2009), 110–113.
21. T. Koizumi, N. Tsujiuchi, R. Akatsuka, Analysis of interaction between grouser and soil using distinct element method (DEM), *J. Syst. Des. Dynam.*, **4** (2010), 914–927.
22. F. Wakui, Y. Terumichi, Three-dimensional numerical simulation of tire behavior on soft ground, *Trans. Jpn. Soc. Mech. Eng.*, **77** (2011), 3264–3277.
23. Y. Wang, *The Analysis of the Interaction Between Wheel and Soft Ground Based on DEM*, Doctoral dissertation, Jilin University, 2012.
24. F. Liu, *Research on Dynamic Simulation System of the Interaction Between Irregular Structure Wheel and Loose Lunar Soil Simulant*, Doctoral dissertation, Jilin University, 2013.
25. R. Zhang, Bionic design of configuration of rigid wheel moving on sand and numerical analysis on its traction performance, *Trans. Chin. Soc. Agri. Eng.*, **31** (2015), 122–128.
26. W. Smith, D. Melanz, C. Senatore, Comparison of discrete element method and traditional modeling methods for steady-state wheel-terrain interaction of small vehicles, *J. Terramech.*, **56** (2014), 61–75.
27. R. Shi, *Research on Influencer of Low Gravity to Mechanical Properties of Lunar Soil Simulant and Interaction Between Lunar Soil Simulant and Lunar Rover*, Doctoral dissertation, Jilin University, 2014.
28. C. Zhao, M. Zang, Analysis of rigid tire traction performance on a sandy soil by 3D finite element-discrete element method, *J. Terramech.*, **55** (2014), 29–37.
29. J. Johnson, A. Kulchitsky, P. Duvoy, Discrete element method simulations of Mars exploration rover wheel performance, *J. Terramech.*, **62** (2015), 31–40.
30. X. Li, *Analysis of Tractive Performance for Wheel on Sandy Road Using Discrete Element Method*, Doctoral dissertation, National University of Defense Technology, 2015.
31. Y. Du, J. Gao, L. Jiang, Numerical analysis of lug effects on tractive performance of off-road wheel by DEM, *J. Braz. Soc. Mech. Sci. Eng.*, **39** (2017), 1977–1987.
32. K. Nishiyama, H. Nakashima, H. Shimizu, 2D FE-DEM analysis of contact stress and tractive performance of a tire driven on dry sand, *J. Terramech.*, **74** (2017), 25–33.
33. S. Kumar, Effect of ballasting on performance characteristics of bias and radial ply tyres with zero sinkage, *Measurement*, **121** (2018), 218–224.
34. R. Kumar, Deflection characteristics for radial-ply tractor tyres, *J. Pharmacogn. Phytochem.*, **7** (2018), 2016–2021.
35. J. F. Peters, F. Vahedifard, B. Jelinek, G. Mason, In *The discrete element method for vehicle-terrain analysis*, Proceedings of the 15th European-African Regional Conference of the International Society for Terrain-Vehicle Systems, Prague, 2019.
36. S. Kumar, Performance characteristics of mode of ballast on energy efficiency indices of agricultural tyre in different terrain condition in controlled soil bin environment, *Energy*, **182** (2019), 48–56.
37. G. Wang, W. Hao, J. Wang, *Discrete Element Method and Its Practice in EDEM*, Northwestern Polytechnical University Press, Xi'an, (2010), 26–74.

38. P. Jayakumar, D. Melanz, J. Maclennan, Scalability of classical terramechanics models for lightweight vehicle applications incorporating stochastic modeling and uncertainty propagation, *J. Terramech.*, **54** (2014), 37–57.
39. C. Senatore, K. Iagnemma, Analysis of stress distributions under lightweight wheeled vehicles, *J. Terramech.*, **51** (2014), 1–17.
40. J. Y. Wong, A. R. Reece, Prediction of rigid wheel performance based on the analysis of soil-wheel stresses: Part I: Performance of driven rigid wheels, *J. Terramech.*, **4** (1967), 81–98.
41. GB/T50123-1999, *Industrial Standards of the People's Republic of China*, Standard for Soil Test Method, 1999.
42. L. Shi, W. Zhao, W. Sun, Parameter calibration of soil particles contact model of farmland soil in northwest arid region based on discrete element method, *Trans. Chin. Soc. Agri. Eng.*, **33** (2017), 181–187.
43. R. Zhang, T. Han, Q. Ji, Y. He, J. Li, Calibration methods of sandy soil parameters in simulation of discrete element method, *J. Agri. Mach.*, **48** (2017), 49–56.
44. Y. Du, J. Gao, L. Jiang, Numerical analysis on tractive performance of off-road wheel steering on sand using discrete element method, *J. Terramech.*, **71** (2017), 25–43.
45. Y. He, W. Xiang, M. Wu, Parameters calibration of loam soil for discrete element simulation based on the repose angle of particle heap, *J. Hunan. Agri. Univ.*, **44** (2018), 216–220.
46. J. Li, J. Tong, B. Hu, Calibration of parameters of interaction between clayey black soil with different moisture content and soil-engaging component in northeast China, *Trans. Chin. Soc. Agri. Eng.*, **35** (2019), 130–140.



AIMS Press

©2020 the Author(s), licensee AIMS Press. This is an open access article distributed under the terms of the Creative Commons Attribution License (<http://creativecommons.org/licenses/by/4.0>)